

Self-Supervised Learning for SAR ATR with a Knowledge-Guided Predictive Architecture

Weijie Li, Yang Wei*, Tianpeng Liu, Yuenan Hou, Yongxiang Liu*, Li Liu*,

Abstract—Recently, the emergence of a large number of Synthetic Aperture Radar (SAR) sensors and target datasets has made it possible to unify downstream tasks with self-supervised learning techniques, which can pave the way for building the foundation model in the SAR target recognition field. The major challenge of self-supervised learning for SAR target recognition lies in the generalizable representation learning in low data quality and noise. To address the aforementioned problem, we propose a knowledge-guided predictive architecture that uses local masked patches to predict the multiscale SAR feature representations of unseen context. The core of the proposed architecture lies in combining traditional SAR domain feature extraction with state-of-the-art scalable self-supervised learning for accurate generalized feature representations. The proposed framework is validated on various downstream datasets, *i.e.*, MSTAR, FUSAR-Ship, SAR-ACD and SSD, and can bring consistent performance improvement for SAR target recognition. The experimental results strongly demonstrate the unified performance improvement of the self-supervised learning technique for SAR target recognition across diverse targets, scenes and sensors.

Index Terms—Synthetic Aperture Radar (SAR), Automatic Target Recognition (ATR), Self-Supervised Learning, Deep Learning, Masked Autoencoder

1 INTRODUCTION

SYNTHETIC aperture radar (SAR) has been indispensable for acquiring information in Earth observation [1, 2, 3], with its stable imaging capability in almost all weather and light conditions. The imaging principle of SAR is Fourier optics and imaging, which implies computational imaging by transmitting and receiving a series of echo signals from a moving platform, such as an airborne or satellite-based radar. Therefore, SAR imaging is significantly different from visible light imaging in terms of imaging planes and mechanisms. SAR images have speckle noise, phase error, geometric distortion, and other special properties [1, 2], and these unique properties present significant challenges for SAR image interpretation. As an important role in SAR image interpretation, SAR Automatic Target Recognition (ATR) aims to automatically confirm information such as the location and category of the interested target in a SAR image by computer. It has been studied extensively over the past decades and has various civilian and military applications, including transportation management [4], automatic driving [5], concealment detection [6], and military reconnaissance [7, 8].

In the last decade, deep learning has reinvigorated and made impressive progress in SAR target recognition with its scalable ability to learn the corresponding feature representations from different data [9, 10, 11]. Although great breakthroughs have been made in this field, SAR target recognition studies are divided into several subfields due to dataset factors, such as vehicle [7], ship [12], and aircraft [13] recognition. Therefore, an interesting and worthwhile question to explore is *whether there*

*This work was partially supported by the National Key Research and Development Program of China No. 2021YFB3100800, and the National Natural Science Foundation of China under Grant 61871384, 61921001, 62022091, and 62201588 and 62376283, and the Science and Technology Innovation Program of Hunan Province under Grant 2022RC1092. (*Corresponding author: Yang Wei, Yongxiang Liu, and Li Liu.)*

Weijie Li, Yang Wei, Tianpeng Liu, Yongxiang Liu, Li Liu are with the College of Electronic Science and Technology, National University of Defense Technology, Changsha, 410073, China (e-mail: lwj2150508321@sina.com, yw850716@sina.com, everliutianpeng@sina.cn, lyx_bible@sina.com, and dreamliu2010@gmail.com).

Yuenan Hou is with the Shanghai AI Laboratory, Shanghai, 200000, China (e-mail: houyuenan@pjlab.org.cn).

exists a uniform and generalized feature representation for various SAR recognition tasks.

The developing SAR datasets and self-supervised learning techniques show the path to solving this problem. As shown in Fig. 1, new datasets have emerged in the last three years, greatly enriching the SAR target dataset and providing a data foundation for studying the problem. Moreover, self-supervised learning [14, 15] techniques have demonstrated the ability to generalize to downstream tasks from a large number of samples, such as computer vision [16, 17], remote sensing [18], clinical medical [19]. Therefore, we believe that a uniform and generalized feature representation for SAR target recognition can be learned from a large dataset by self-supervised learning techniques. However, due to the unique imaging mechanisms in the SAR field, the main fundamental challenges of self-supervised learning for SAR ATR are summarized and discussed briefly in the following.

Lack of a large-scale pre-training set. Just as ImageNet [20] has achieved a qualitative change in computer vision by pushing the number of categories for object recognition in computer vision from twenty to thousands, a large-scale pre-training set for SAR target recognition will bring new research ideas: generalized features from subfield to real-world level. Unfortunately, due to the acquisition cost and annotation difficulties, most current SAR target datasets have at most ten annotation categories and a few thousand images. Whereas some studies [21, 22] in SAR target recognition have used a few datasets as pre-training and downstream tasks, the potential of self-supervised learning in large-scale SAR datasets has yet to be explored. Therefore, it is necessary to integrate different publicly available datasets to construct a large-scale pre-training set containing diverse targets, scenes, and sensors¹.

Special properties of SAR images. SAR achieves coherent imaging through a moving platform, and two-dimensional SAR images reflect the information through the orientation dimension

¹ Various imaging conditions regarding target, scene, and sensor can lead to complex target and background signature variations in SAR images [7, 23].

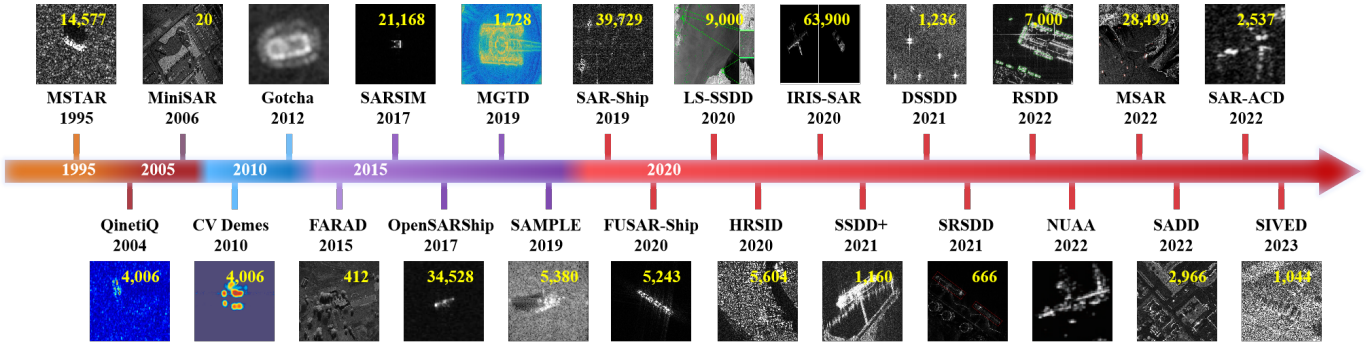


Fig. 1: Timeline of simulated and measured datasets for SAR target recognition. From the figure, we can see that vehicle targets dominate the early stage. A rapid increase in new SAR target datasets in the 2020s has greatly enriched the target, scene, and sensor diversity of SAR target datasets. However, the number of images in most datasets is only a few thousand due to the high costs and difficult annotation.

(the direction of motion) and the oblique distance dimension (the direction of the vertical orientation dimension). Its imaging plane is significantly different from visible light imaging, and the SAR image reflects the electromagnetic scattering characteristics of the object. Therefore, SAR image interpretation is extremely difficult due to the huge differences from human vision. Besides, multiplicative speckle noise, phase error, and other interference can impact the imaging results and reduce the image quality. These properties challenge the self-supervised learning methods, and we found that the masked autoencoders (MAE) [17] reconstruct the original pixels with noise interference, Masked Feature Prediction (MaskFeat) [24] uses hog features unsuitable for SAR images, and Image-based Joint-Embedding Predictive Architecture (I-JEPA) [25] undergoes feature collapse due to image quality. Furthermore, various data augmentation pretext tasks [26] in self-supervised learning are not fully suitable for SAR images; for example, the rotated SAR image does not truly reflect the rotation of the sensor's imaging plane. Therefore, it is indispensable to combine self-supervised learning and SAR domain knowledge to solve these special problems.

In order to deploy self-supervised learning for SAR target recognition, we construct a large pre-training set containing nearly 100,000 images² based on four publicly available datasets (MSAR [27, 28], SAR-Ship-Dataset [29], SARSIM [30, 31], and SAMPLE [32]) in Fig. 1. This pre-training set contains diverse target classes, scenes and sensors to explore effective self-supervised learning methods. Moreover, we use four other classification and detection datasets (MSTAR [33], FUSAR-Ship [12], SAR-ACD [34], SSDD [35]) as downstream tasks to evaluate the generalization performance. In summary, we establish a self-supervised learning benchmark for SAR recognition and propose our method for the speckle noise and target scale problems in SAR images.

As illustrated in Fig. 2, a knowledge-guided predictive architecture (KGPA) is proposed to leverage SAR domain knowledge and the meaningful masked image modeling task to learn contextual relationships in a SAR feature space. Inspired by the physics-guided contrastive architecture [11] and local descriptors for target recognition [36] in SAR domain, we use classical feature extraction method (gradient by ratio [37, 38]) as target encoder to solve the speckle noise in SAR images and extract the edge shape information of the targets. In addition, since small multi-scale targets in remote sensing are easily obscured by masks, we propose local multi-scale features to

accommodate better the target scale under remote sensing vision. In the end, the proposed architecture is validated on various downstream datasets with widely improved performance for SAR target recognition.

The main contributions of this article are summarized as follows:

- Our experiments show that the performance of the self-supervised learning model benefits from a large-scale dataset under various SAR target recognition datasets.
- We proposed a physics-guided contrastive architectures to leverage SAR domain knowledge and masked image modeling task, which achieves better performance in various downstream datasets. Our study shows that employing SAR domain knowledge for the unique properties of SAR images is key to ensuring the generalization features of self-supervised learning.
- As the first large-scale pre-training study in SAR target recognition, our work will stimulate the research enthusiasm for the unified feature representation and fundamental models for SAR target recognition.

The remainder of this paper is organized as follows. Sec. ?? introduces related studies in self-supervised learning and SAR target recognition. Sec. 2 introduces the proposed knowledge-guided predictive architecture. Sec. 3 conducts extensive experiments to demonstrate the performance of our method. Sec. ?? concludes the whole paper.

2 APPROACH

The proposed knowledge-guided predictive architecture for SAR target recognition (SAR-KGPA) is illustrated in Fig. 3. Our overall objective is as follows: given local masked patches, predict feature representation for SAR domain knowledge. By predicting local masked patches in a diverse pre-training set, the model can achieve SAR image interpretation by recognizing the contextual relationship between target parts and the surrounding area.

The architecture flow is shown in Fig. 3, and the input is the single-channel SAR magnitude image since most target datasets are magnitude pictures. Then, we randomly select different local patches and add mask tokens according to Local Masked Reconstruction (LoMaR) [39]. We use a Vision Transformer (ViT) [40] in MAE as the DNN-encoder and DNN-predictor. Each local masked patch is fed into the MAE structure to predict the target feature of mask tokens.

2. Since most SAR target datasets are magnitude images, the pre-training set is comprised of SAR magnitude images.

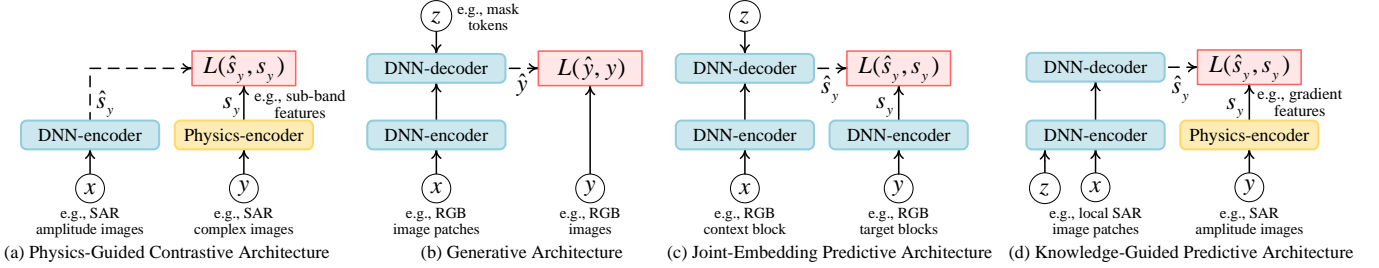


Fig. 2: Architectures for self-supervised learning, in which the different pretext tasks add implicit constraints. (a) Physics-guided contrastive architectures use the physical representation of SAR images as a guided signal that constrains the feature representation of the Deep Neural Network (DNN). (b) Generative architectures reconstruct the pixels of the image with a high mask proportion, yielding a nontrivial and meaningful pretext task to learn contextual relationships within images. (c) Joint-embedding predictive architecture aims to predict in a learnable feature space to obtain semantic representations. (d) Knowledge-guided predictive architectures combine leverage SAR domain knowledge and the meaningful pretext task to learn contextual relationships in a SAR feature space.

Importantly, due to the large differences between SAR and RGB images, predicting target features requires SAR domain knowledge. SAR coherent imaging results in multiplicative scattering noise in the magnitude image, so we use the gradient by ratio [37, 38] to suppress the speckle noise and extract the targets' edge and shape information. Moreover, we employ a multi-scale convolutional kernel instead of a single scale for multi-scale targets in the pre-training set.

2.1 Local Masked Patches

We aim to learn the contextual relationship between the target parts and their scenes. Whereas such relationships normally remain in small areas due to the large scale and small target for remote sensing imagery. Therefore, MAE reconstructing each missing patch with patches easily removes the small target area, and we perform masking in the local patches following LoMaR. Although LoMaR is designed to improve computational efficiency, we find this local setting is suited for small targets in remote sensing. According to the LoMaR [39], mask tokens and relative positional encoding [41] are added to the encoder input and MAE structure to enhance the feature representation.

2.2 Target Encoder

Due to the SAR imaging mechanism [2], the images' amplitude values contain multiplicative speckle noise. The speckle noise is related to the sensor resolution and is caused by the coherent superposition of different scatterers within the scattering cell. Therefore, reconstructing image pixels for SAR images receives noise interference and fails to learn a high-quality feature representation. This problem of speckle noise can be solved by filtering and feature extraction. However, filtering has a conflict between noise reduction and image details, and we use feature extraction. Some studies have proposed different types of target features in computer vision, mainly divided into traditional manual features [24] and deep learning features [25]. However, these methods are difficult to migrate to SAR target recognition directly, so we combine the traditional local description feature extraction methods [36, 37, 38] in the SAR domain.

Gradient by ratio. The classical difference gradient is not a constant false alarm rate operator due to multiplicative speckle noise in the SAR image, and previous studies [42, 43] have shown that the computing ratio is more suitable for multiplicative noise. Here, we use the simplest ratio of average (ROA) [42] to not blur image details:

$$R_i = \frac{M_1(i)}{M_2(i)}, \quad (1)$$

where R_i denotes the ratio of average at different directions and $M_1(i)$ and $M_2(i)$ are the area averages on opposite sides of the current pixel along direction i . $i = 1$ is the horizontal direction and $i = 3$ means the vertical direction. As shown in Fig. 3, the area averages can be computed from the image and four fixed convolution kernels.

The use of logarithms can solve the vertical gradient calculation [37], and the horizontal and vertical gradients are defined as:

$$\begin{aligned} G_H &= \log(R_1), \\ G_V &= \log(R_3), \end{aligned} \quad (2)$$

where G_H is the horizontal gradient and G_V is the vertical gradient. The gradient magnitude is $G_m = \sqrt{G_H^2 + G_V^2}$,

Multi-Scale Feature. Previous study [38] has discussed the impact of different convolutional kernel sizes for SAR vehicle target recognition. Therefore, when the pre-training set is extended to various target categories with different sizes, a multi-scale feature pyramid needs to be constructed with convolutional kernels of different scales.

2.3 Implementation

Given an SAR image, we randomly sample several square windows at different spatial locations as local patches and mask each patch with mask tokens at a fixed percentage. Then, each local patch's visible and masked ones are fed into the MAE structure, whose encoder and predictor are applied with learnable relative positional encoding in the self-attention layer. Meanwhile, the whole SAR image is provided to the target encoder. The average values in four directions are obtained after multi-scale convolution in four directions. Then, the gradients by ratio are obtained as multi-scale SAR features by the ratio and logarithm operations. The loss function computes the mean squared error (MSE) between the DNN features and SAR multi-scale features only at masked patches in the feature space. Although our code is based on MAE and LoMaR, in addition to the major improvement of the target encoder, there are two other minor as follows.

Data augmentation. We follow the simple data augmentations in MAE (random resize and horizontal flipping) and add random contrast augmentation for SAR magnitude images.

Decoder design. While some work [24, 39] has shown that it is feasible to use a simple linear head as a decoder or predictor for self-supervised learning in RGB images, we find that a ViT with eight layers in the MAE is less disturbed by SAR image noise than a linear layer, allowing the encoder to extract deep semantic features of targets.

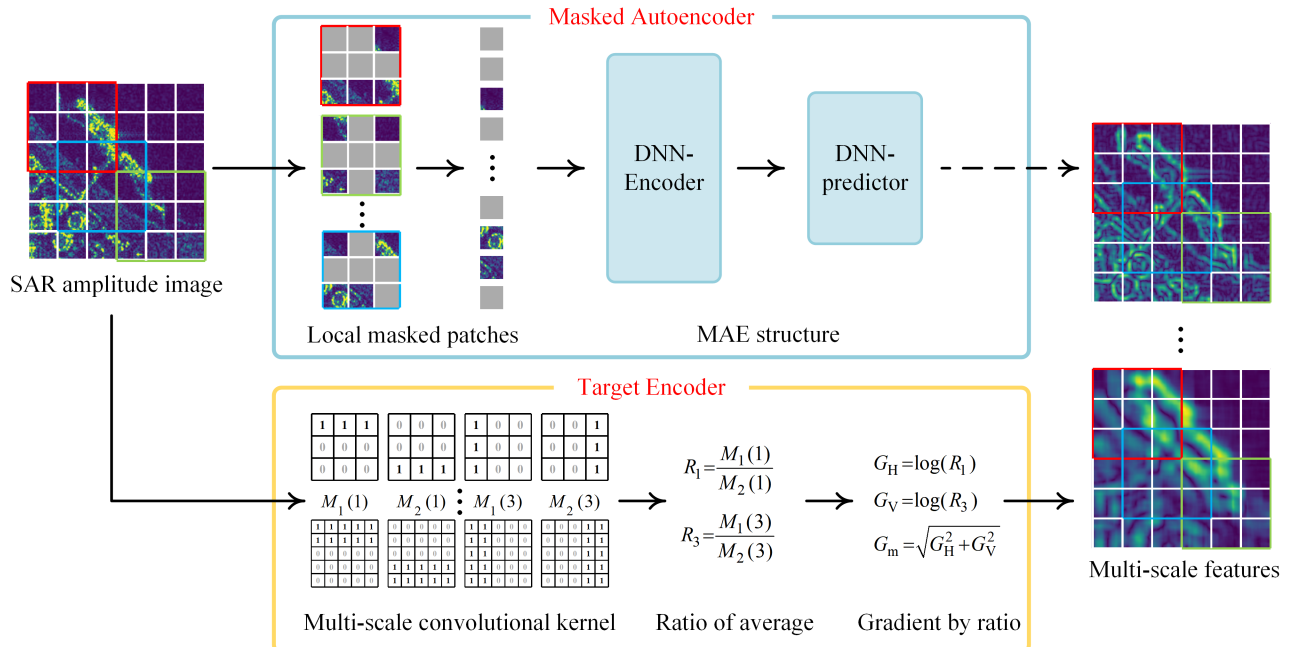


Fig. 3: SAR-KGPA. The proposed knowledge-guided predictive architecture for SAR target recognition uses local masked patches to predict the multiscale SAR feature representations of unseen contexts. The MAE structure uses the Vision Transformer (ViT). DNN-encoder extracts deep features of masked patches, and DNN-predictor predicts SAR features of unseen contexts. The target-encoder uses the gradient by ratio to map SAR images from pixel space to feature space, thus avoiding speckle noise interference in SAR images. Local patches and multiscale features are designed for multiscale small targets in remote sensing.

3 EXPERIMENTS

3.1 Dataset and Experimental Settings

Since diverse targets, scenes, and sensor parameters constitute a large data sampling space in real-world situations, constructing a rich pre-training is central to unifying various target recognition tasks. Although SAR target datasets have been enriched recently (mostly ship targets), no single dataset contains all popular target categories (vehicles, ships, and aircraft) and various image conditions. As shown in Table 1 and Fig. 4, we used four datasets constituting a large pre-training set containing different target types, scenes, and sensors. Self-supervised learning models are tested on other common target recognition datasets to evaluate the ability of fine-grained semantic information extraction in small sample situations and target localization in large scenarios. The datasets' details are described as follows.

3.1.1 Pre-training dataset

Pre-training datasets are designed to ensure rich information about targets, scenes, and sensors. Therefore, we chose four datasets covering popular targets (vehicles, ships, aircraft, etc), complex backgrounds (ground and ocean), and various sensors (satellite-borne, airplane-borne, and simulation).

MSAR [27, 28] is a multi-class target detection dataset based on the Chinese HISEA-1 satellite in large-scale scenes. MSAR comprises 28,449 image slices with quad polarization. Scenes covered include airports, harbors, nearshore, islands, distant seas, urban areas, etc. The labeled target categories include aircraft, oil tanks, bridges, and ships. This dataset can provide target samples in complex ground and sea scenes.

SAR-Ship-Dataset [29] is a ship target detection dataset in complex scenes based on Chinese Gaofen-3 and European Sentinel-1 satellites. The public version of this dataset contains 39,729 images from two satellites in different imaging modes and resolutions. The dataset provides ship targets of various sizes in

complex ocean scenes such as nearshore, distant seas, harbors, and islands.

SARSim [30, 31] is a fine-grained vehicle dataset created by Terma A/S, Denmark. The simulation system used for this dataset can generate X-band SAR images with resolutions ranging from 0.1m to 0.3m from CAD models. SARSim provides 21,168 vehicle samples in 7 categories (truck, car, motorbike, bus, tank, bulldozer, and pickup) and 3 scenes (grass, roads, and a mean of the two) with 7 imaging depression angles. This dataset provides fine-grained differences between vehicles.

SAMPLE [32] is a fine-grained synthetic and measured paired vehicle dataset released by the Air Force Research Laboratory, USA. This dataset is simulated in X-band and 0.3m resolution. The public version of this dataset provides 5,380 images of ten categories of military vehicle targets at partial imaging angles, and five categories overlap with the public version of MSTAR. As shown in Fig. 4, it can be noticed that the ground clutter in SAMPLE is more significant and realistic than in SARSim.

3.1.2 Downstream tasks

We selected other target recognition datasets to evaluate the generalization of self-supervised learning better. The downstream datasets include various fine-grained targets (vehicles, ships, and aircraft) and different task (classification and detection) to evaluate the performance of self-supervised learning for SAR target recognition comprehensively.

MSTAR [33] is the most commonly used SAR target classification dataset released by the Defense Advanced Research Projects Agency, USA, which contains ten categories of military vehicles with different angles, variants, and other imaging conditions. It has many experimental setup variants, while we refer to the [44] to adopt the most commonly used ten-class classification settings to evaluate the fine-grained classification performance for SAR vehicles.

TABLE 1: Description of SAR datasets used for pre-training and downstream tasks. # Target: Number of target categories. # Scene: Number of scene. Res.: Resolution. Large SAR imagery in the detection contains more target and scene types than the annotation.

Dataset	Size	# Target	# Scene	Res. (m)	Band	Polarization	Description
MSAR [27, 28]	28,499	≥ 4	≥ 6	1	C	Quad	Ground and sea targets detection dataset
SAR-Ship-Dataset [29]	39,729	≥ 1	≥ 4	3~25	C	Quad	Ship detection dataset in complex scenes
SARSim [30, 31]	21,168	7	3	0.3	X	Single	Vehicle simulation dataset
SAMPLE [32]	5,380	10	1	0.3	X	Single	Vehicle simulation and measured dataset
MSTAR [33]	5,216	10	1	0.3	X	Single	Fine-grained vehicle classification dataset
FUSAR-Ship [12]	9,830	10	≥ 5	1.1~1.7	C	Double	Fine-grained ship classification dataset
SAR-ACD [34]	2,537	6	3	1	C	Single	Fine-grained aircraft classification dataset
SSDD [35]	1,160	1	≥ 2	1~15	C/X	Quad	Common ship detection dataset

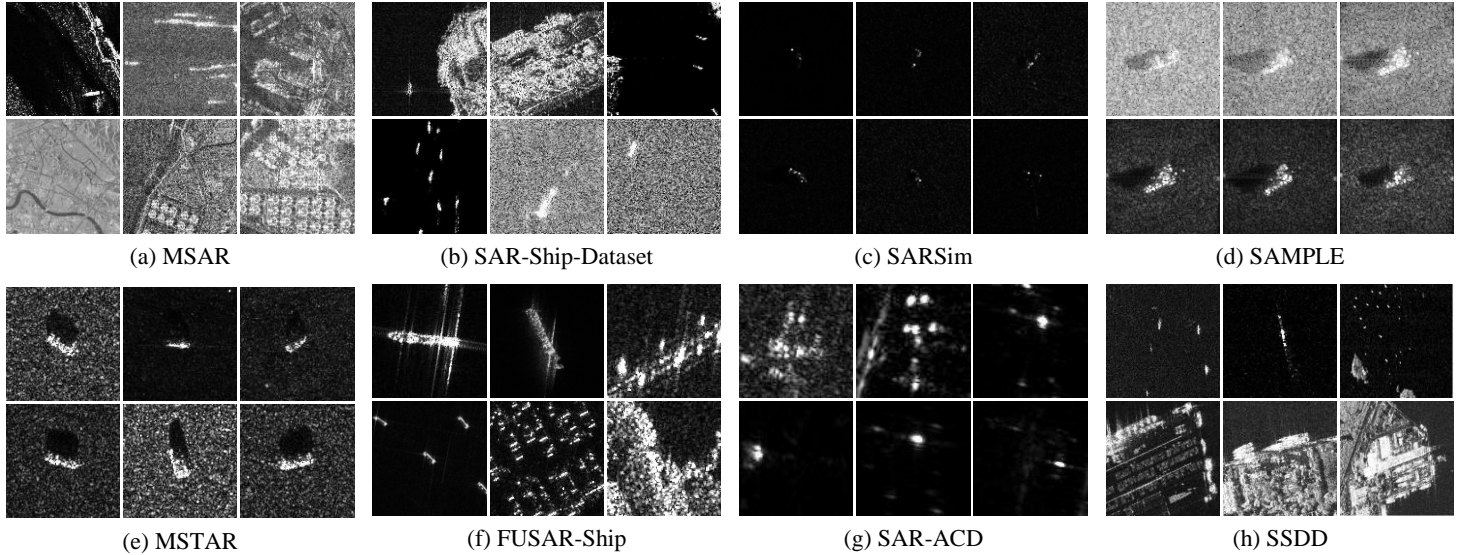


Fig. 4: The datasets for the self-learning and downstream tasks contain various targets, scenes, and sensors. The first row is the datasets used for self-learning; MSAR is the satellite-based dataset of ground and sea targets; SAR-Ship-Dataset is the satellite-based dataset of sea targets; SARSim is the multi-angle simulation dataset of vehicle targets, and SAMPLE is the simulated and measured dataset. The second row is the downstream dataset; MSTAR is the spotlight SAR image classification of vehicle targets; FUSAR-Ship is the satellite-based SAR image classification of sea targets; SAR-ACD is the satellite-based SAR image classification of aircraft targets; SSDD is the satellite-based SAR image detection of sea targets.

FUSAR-Ship [34] contains 15 primary ship categories and many non-ship targets based on the Gaofen-3 satellite in scenes such as sea, land, coast, river, and island. Based on the experimental setup of [45], we have ten types of ocean targets, such as fine-grained ships, bridges, and ocean scene slices. We use this dataset to evaluate the fine-grained classification performance for the ocean targets.

SAR-ACD [34] contains six types of aircraft based on the Gaofen-3 satellite in three civil airports, including Shanghai Hongqiao Airport, Beijing Capital Airport, and Taiwan Taoyuan Airport. Since the released dataset does not separate the training and test data, we randomly select small samples as the training set and others as the test set. We use this dataset to evaluate the benefit of the pre-training methods for fine-grained aircraft target classification. Fine-grained recognition of aircraft targets is a more challenging task due to the smooth surface of the aircraft, resulting in insignificant features.

SSDD [35] is a commonly used SAR detection dataset. It is constructed based on Canadian RadarSat-2, German TerraSAR-X, and European Sentinel-1 satellites and contains different scenarios for the inshore and offshore of China and India. The dataset covers different ship sizes in different oceanic conditions with diverse clutter and scattered noise interference. We use this dataset to evaluate the improvement of pre-trained models for target localization in SAR remote sensing.

3.1.3 Experimental Settings

With the following procedure, we examine self-supervised learning performance based on the eight mentioned datasets. First, we perform the self-supervised learning on the pre-training dataset without label information. The pre-training is applied on 4 NVIDIA V100 GPUs with 200 epochs and 300 batch sizes, and the backbone model is ViT-Base. Then, we finetune the pretrained model on SAR classification and detection datasets. Detailed settings and hyperparameters are in the supplementary material and our GitHub.

3.2 Results

Table 2 summarizes the results for downstream SAR recognition datasets. Self-supervised learning allows ViT to learn the inductive bias in SAR images and apply them to different downstream datasets, with improved performance on the small-sample SAR classification task and higher target localization accuracy in the SAR detection task. By comparing different pre-training methods, we have the following three findings.

SAR vs. RGB. Due to the large discrepancy between SAR imaging and visible optical imaging, pre-training with SAR images can achieve better results with a smaller sample size than pre-training on RGB images. Even ImageNet21k weights pre-trained on 10 million RGB images do not perform as well in

TABLE 2: SAR image classification and detection results. ImageNet refers to pre-training on ImageNet21k in supervised learning, and other self-supervised learning methods are applied to the SAR pre-training set. Their backbone is ViT-Base. MSTAR is a vehicle dataset. FUSAR-Ship and SSDD are Ship datasets. SAR-ACD is an aircraft Dataset. The classification metric is accuracy, and the detection metric is AP_{50} . **Bold** indicates the best result, underline indicates the next best result.

Method	Classification									Detection SSDD	
	MSTAR (10 classes)			FUSAR-Ship (10 classes)			SAR-ACD (6 classes)				
	10-shot	20-shot	40-shot	10-shot	20-shot	40-shot	10-shot	20-shot	40-shot		
No Pre-training	20.32	25.74	28.78	45.58	47.72	55.16	28.04	46.66	51.66	90.5	
ImageNet	37.68	48.64	57.62	75.74	80.32	82.66	43.70	43.88	63.14	89.5	
MAE	49.56	60.78	72.48	77.66	80.70	83.90	53.94	60.34	71.90	91.1	
LoMaR	50.58	64.72	80.56	80.84	84.72	88.44	55.24	61.94	72.64	92.1	
SAR-KGPA	70.04	82.98	89.98	86.22	87.80	90.60	57.84	65.98	75.70	92.8	

SAR downstream recognition tasks as weights pre-trained on 94 thousand SAR images.

Small targets in remote sensing. The small target foreground occupies a small percentage of the image for remote sensing, such as aerial and satellite. Therefore, local masking patches are more suitable for learning the contextual information of small targets and surrounding regions in remote sensing images, and our masking method is based on LoMaR instead of MAE.

SAR domain knowledge effectively guides feature representation learning. SAR imaging suffers from multiplicative speckle noise, foreshortening, layover, shadow, and other unique phenomena that result in poor image quality. Therefore, it is essential to combine traditional feature extraction and domain knowledge to guide deep learning. Our architecture uses the successful gradient extraction method in the SAR domain to address the interference of multiplicative speckle noise in SAR magnitude images, thus achieving the best performance. In the next subsection, we further analyze the problem of target feature selection for self-supervised learning.

Our experiments show that it is time to embrace self-supervised learning to take advantage of the growing SAR target samples. The large pre-training samples gives self-supervised learning the potential to achieve a unified and stable feature representation for various downstream tasks across targets, scenes, and sensors.

REFERENCES

[1] G.-C. Sun, Y. Liu, J. Xiang, W. Liu, M. Xing, and J. Chen, "Spaceborne synthetic aperture radar imaging algorithms: An overview," *IEEE Geosci. Remote Sens. Mag.*, vol. 10, no. 1, pp. 161–184, 2021.

[2] A. Moreira, P. Prats-Iraola, M. Younis, G. Krieger, I. Hajnsek, and K. P. Papathanassiou, "A tutorial on synthetic aperture radar," *IEEE Geosci. Remote Sens. Mag.*, vol. 1, no. 1, pp. 6–43, 2013.

[3] A. Tsokas, M. Rysz, P. M. Pardalos, and K. Dipple, "SAR data applications in earth observation: An overview," *Expert Syst. Appl.*, vol. 205, p. 117342, 2022.

[4] V. Gagliardi, F. Tosti, L. Bianchini Ciampoli, M. L. Battagliere, L. D'Amato, A. M. Alani, and A. Benedetto, "Satellite remote sensing and non-destructive testing methods for transport infrastructure monitoring: Advances, challenges and perspectives," *Remote Sens.*, vol. 15, no. 2, p. 418, 2023.

[5] M. Rizzi, D. Tagliaferri, S. Tebaldini, M. Nicoli, I. Russo, C. Mazzucco, A. V. Monti-Guarnieri, C. M. Prati, and U. Spagnolini, "Navigation-aided automotive SAR imaging in urban environments," in *Proc. Int. Geosci. Remote. Sens. Symp. (IGARSS)*. IEEE, 2021, pp. 2979–2982.

[6] P.-O. Frolind, A. Gustavsson, M. Lundberg, and L. M. Ulander, "Circular-aperture VHF-band synthetic aperture radar for detection of vehicles in forest concealment," *IEEE Trans. Geosci. Remote Sens.*, vol. 50, no. 4, pp. 1329–1339, 2011.

[7] W. Li, W. Yang, W. Zhang, T. Liu, Y. Liu, and L. Liu, "Hierarchical disentanglement-alignment network for robust SAR vehicle recognition," *IEEE J. Sel. Top. Appl. Earth Obs. Remote Sens.*, vol. 16, pp. 9661–9679, 2023.

[8] B. Peng, B. Peng, J. Zhou, J. Xie, and L. Liu, "Scattering model guided adversarial examples for SAR target recognition: Attack and defense," *IEEE Trans. Geosci. Remote Sens.*, vol. 60, pp. 1–17, 2022.

[9] O. Kechagias-Stamatis and N. Aouf, "Automatic target recognition on synthetic aperture radar imagery: A survey," *IEEE Aerosp. Electron. Syst. Mag.*, vol. 36, no. 3, pp. 56–81, 2021.

[10] J. Li, Z. Yu, L. Yu, P. Cheng, J. Chen, and C. Chi, "A comprehensive survey on SAR ATR in deep-learning era," *Remote Sens.*, vol. 15, no. 5, p. 1454, 2023.

[11] M. Datcu, Z. Huang, A. Anghel, J. Zhao, and R. Cacoveanu, "Explainable, physics-aware, trustworthy artificial intelligence: A paradigm shift for synthetic aperture radar," *IEEE Geosci. Remote Sens. Mag.*, vol. 11, no. 1, pp. 8–25, 2023.

[12] X. Hou, W. Ao, Q. Song, J. Lai, H. Wang, and F. Xu, "FUSAR-Ship: Building a high-resolution SAR-AIS matchup dataset of Gaofen-3 for ship detection and recognition," *Sci. China Inf. Sci.*, vol. 63, pp. 1–19, 2020.

[13] Y. Zhao, L. Zhao, Z. Liu, D. Hu, G. Kuang, and L. Liu, "Attentional feature refinement and alignment network for aircraft detection in SAR imagery," *IEEE Trans. Geosci. Remote Sens.*, vol. 60, pp. 1–16, 2022.

[14] X. Liu, F. Zhang, Z. Hou, L. Mian, Z. Wang, J. Zhang, and J. Tang, "Self-supervised learning: Generative or contrastive," *IEEE Trans. Knowl. Data Eng.*, vol. 35, no. 1, pp. 857–876, 2021.

[15] R. Balestrieri, M. Ibrahim, V. Sobal, A. Morcos, S. Shekhar, T. Goldstein, F. Bordes, A. Bardes, G. Mialon, Y. Tian *et al.*, "A cookbook of self-supervised learning," *arXiv preprint*, 2023. [Online]. Available: <https://arxiv.org/abs/2304.12210>

[16] M. Goldblum, H. Souri, R. Ni, M. Shu, V. U. Prabhu, G. Somepalli, P. Chattopadhyay, M. Ibrahim, A. Bardes, J. Hoffman, R. Chellappa, A. G. Wilson, and T. Goldstein, "Battle of the backbones: A large-scale comparison of pretrained models across computer vision tasks," in *Proc. Adv. Neural Inf. Process. Syst. (NeurIPS)*, 2023. [Online].

Available: <https://openreview.net/forum?id=1yOnfDpkVe>

[17] K. He, X. Chen, S. Xie, Y. Li, P. Dollár, and R. Girshick, "Masked autoencoders are scalable vision learners," in *Proc. IEEE Comput. Soc. Conf. Comput. Vis. Pattern Recognit. (CVPR)*, 2022, pp. 16 000–16 009.

[18] X. Sun, P. Wang, W. Lu, Z. Zhu, X. Lu, Q. He, J. Li, X. Rong, Z. Yang, H. Chang, Q. He, G. Yang, R. Wang, J. Lu, and K. Fu, "RingMo: A remote sensing foundation model with masked image modeling," *IEEE Trans. Geosci. Remote Sens.*, vol. 61, pp. 1–22, 2023.

[19] Y. Zhou, M. A. Chia, S. K. Wagner, M. S. Ayhan, D. J. Williamson, R. R. Struyven, T. Liu, M. Xu, M. G. Lozano, P. Woodward-Court *et al.*, "A foundation model for generalizable disease detection from retinal images," *Nature*, pp. 1–8, 2023.

[20] L. Fei-Fei and R. Krishna, "Searching for computer vision north stars," *Daedalus*, vol. 151, no. 2, pp. 85–99, 2022.

[21] Z. Huang, X. Yao, Y. Liu, C. O. Dumitru, M. Datcu, and J. Han, "Physically explainable CNN for SAR image classification," *ISPRS J. Photogramm. Remote Sens.*, vol. 190, pp. 25–37, 2022.

[22] Y. Zhai, W. Zhou, B. Sun, J. Li, Q. Ke, Z. Ying, J. Gan, C. Mai, R. D. Labati, V. Piuri, and F. Scotti, "Weakly contrastive learning via batch instance discrimination and feature clustering for small sample SAR ATR," *IEEE Trans. Geosci. Remote Sens.*, vol. 60, pp. 1–17, 2022.

[23] T. D. Ross, J. J. Bradley, L. J. Hudson, and M. P. O'connor, "SAR ATR: So what's the problem? An MSTAR perspective," in *Proc. SPIE Conf. Algorithms SAR Imagery*, vol. 3721, 1999, pp. 662–672.

[24] C. Wei, H. Fan, S. Xie, C.-Y. Wu, A. Yuille, and C. Feichtenhofer, "Masked feature prediction for self-supervised visual pre-training," in *Proc. IEEE Comput. Soc. Conf. Comput. Vis. Pattern Recognit. (CVPR)*, 2022, pp. 14 668–14 678.

[25] M. Assran, Q. Duval, I. Misra, P. Bojanowski, P. Vincent, M. Rabbat, Y. LeCun, and N. Ballas, "Self-supervised learning from images with a joint-embedding predictive architecture," in *Proc. IEEE Comput. Soc. Conf. Comput. Vis. Pattern Recognit. (CVPR)*, 2023, pp. 15 619–15 629.

[26] A. Jaiswal, A. R. Babu, M. Z. Zadeh, D. Banerjee, and F. Makedon, "A survey on contrastive self-supervised learning," *Technologies*, vol. 9, no. 1, p. 2, 2020.

[27] R. Xia, J. Chen, Z. Huang, H. Wan, B. Wu, L. Sun, B. Yao, H. Xiang, and M. Xing, "CRTTransSAR: A visual transformer based on contextual joint representation learning for SAR ship detection," *Remote Sens.*, vol. 14, no. 6, p. 1488, 2022.

[28] J. Chen, Z. Huang, R. Xia, B. Wu, L. Sheng, L. Sun, and B. Yao, "Large-scale multi-class SAR image target detection dataset-1.0," <https://radars.ac.cn/web/data/getData?dataType=MSAR>, 2022.

[29] K. Wang, G. Zhang, and H. Leung, "SAR target recognition based on cross-domain and cross-task transfer learning," *IEEE Access*, vol. 7, pp. 153 391–153 399, 2019.

[30] D. Malmgren-Hansen, A. Kusk, J. Dall, A. A. Nielsen, R. Engholm, and H. Skriver, "Improving SAR automatic target recognition models with transfer learning from simulated data," *IEEE Geosci. Remote Sens. Lett.*, vol. 14, no. 9, pp. 1484–1488, 2017.

[31] A. Kusk, A. Abulaitijiang, and J. Dall, "Synthetic SAR image generation using sensor, terrain and target models," in *Proc. Eur. Conf. Synth. Aperture Radar, EUSAR 2016*. VDE, 2016, pp. 1–5.

[32] B. Lewis, T. Scarnati, E. Sudkamp, J. Nehrbass, S. Rosencrantz, and E. Zelnio, "A SAR dataset for ATR development: the synthetic and measured paired labeled experiment (SAMPLE)," in *Proc. SPIE Conf. Algorithms SAR Imagery*, vol. 10987, 2019, pp. 39–54.

[33] Air Force Research Laboratory, "The air force moving and stationary target recognition database," <https://www.sdms.afrl.af.mil/index.php?collection=mstar>.

[34] X. Sun, Y. Lv, Z. Wang, and K. Fu, "SCAN: Scattering characteristics analysis network for few-shot aircraft classification in high-resolution SAR images," *IEEE Trans. Geosci. Remote Sens.*, vol. 60, pp. 1–17, 2022.

[35] T. Zhang, X. Zhang, J. Li, X. Xu, B. Wang, X. Zhan, Y. Xu, X. Ke, T. Zeng, H. Su *et al.*, "SAR ship detection dataset (SSDD): Official release and comprehensive data analysis," *Remote Sens.*, vol. 13, no. 18, p. 3690, 2021.

[36] G. Dong, H. Liu, and J. Chanussot, "Keypoint-based local descriptors for target recognition in SAR images: A comparative analysis," *IEEE Geosci. Remote Sens. Mag.*, vol. 9, no. 1, pp. 139–166, 2020.

[37] F. Dellinger, J. Delon, Y. Gousseau, J. Michel, and F. Tupin, "SAR-SIFT: a SIFT-like algorithm for SAR images," *IEEE Trans. Geosci. Remote Sens.*, vol. 53, no. 1, pp. 453–466, 2014.

[38] S. Song, B. Xu, and J. Yang, "SAR target recognition via supervised discriminative dictionary learning and sparse representation of the SAR-HOG feature," *Remote Sens.*, vol. 8, no. 8, p. 683, 2016.

[39] J. Chen, M. Hu, B. Li, and M. Elhoseiny, "Efficient self-supervised vision pretraining with local masked reconstruction," *arXiv preprint*, 2022. [Online]. Available: <https://arxiv.org/abs/2206.00790>

[40] A. Dosovitskiy, L. Beyer, A. Kolesnikov, D. Weissenborn, X. Zhai, T. Unterthiner, M. Dehghani, M. Minderer, G. Heigold, S. Gelly *et al.*, "An image is worth 16x16 words: Transformers for image recognition at scale," *arXiv preprint*, 2020. [Online]. Available: <https://arxiv.org/abs/2010.11929>

[41] K. Wu, H. Peng, M. Chen, J. Fu, and H. Chao, "Rethinking and improving relative position encoding for vision transformer," in *Proc. IEEE Comput. Soc. Conf. Comput. Vis. Pattern Recognit. (CVPR)*, 2021, pp. 10 033–10 041.

[42] R. Touzi, A. Lopes, and P. Bousquet, "A statistical and geometrical edge detector for SAR images," *IEEE Trans. Geosci. Remote Sens.*, vol. 26, no. 6, pp. 764–773, 1988.

[43] A. C. Bovik, "On detecting edges in speckle imagery," *IEEE Trans. Acoust. Speech Signal Process.*, vol. 36, no. 10, pp. 1618–1627, 1988.

[44] W. Li, W. Yang, W. Zhang, T. Liu, Y. Liu, and L. Liu, "Hierarchical disentanglement-alignment network for robust SAR vehicle recognition," *IEEE J. Sel. Top. Appl. Earth Obs. Remote Sens.*, 2023.

[45] D. Wang, Y. Song, J. Huang, D. An, and L. Chen, "SAR target classification based on multiscale attention super-class network," *IEEE J. Sel. Top. Appl. Earth Obs. Remote Sens.*, vol. 15, pp. 9004–9019, 2022.